


Circ_0011292 knockdown mitigates progression and drug resistance in PTX-resistant non-small-cell lung cancer cells by regulating miR-433-3p/CHEK1 axis

Ming Jin¹ | Fengping Zhang² | Qiubo Li³ | Ruiqi Xu³ | Ying Liu³ | Yong Zhang³ 

¹Department of Respiratory and Critical Care Medicine, Jingmen No.1 People's Hospital, Jingmen City, China

²Department of Reproductive Medicine Center, Jingmen No.1 People's Hospital, Jingmen City, China

³Department of Oncology, Jingmen No.1 People's Hospital, Jingmen City, China

Correspondence

Yong Zhang, Department of Oncology, Jingmen No.1 People's Hospital, No.67, Xiangshan Road, Dongbao District, Jingmen City, Hubei Province, 448000, PR China.
Email: drzhang08@163.com

Funding information

This work was supported by The Outstanding Young and Middle-aged Scientific and Technological Innovation Team Program of Colleges and Universities in Hubei Province (No. T201819).

Abstract

Background: Non-small-cell lung cancer (NSCLC) is one of the most common malignant tumors on earth. Circular RNAs have been disclosed to be vital regulators in the chemoresistance and development of diverse cancers, including NSCLC. Here, we attempted to explore the function of circ_0011292 in paclitaxel (PTX)-resistant NSCLC cells.

Methods: Quantitative real-time polymerase chain reaction or western blot was performed to detect the expression of circ_0011292, microRNA-433-3p (miR-433-3p), and checkpoint kinase 1 (CHEK1). Ribonuclease R (RNase R) assay was performed to assess the stability of circ_0011292. Cell Counting Kit-8 assay was conducted to evaluate the half maximal inhibitory concentration of PTX and cell viability. Cell proliferation was monitored by Edu incorporation and colony formation assays. Cell cycle and apoptosis were detected by flow cytometry. Transwell assay was implemented to assess cell migration and invasion. Western blot assay was utilized to determine the protein levels. Dual-luciferase reporter assay was carried out to verify the targeted interaction between miR-433-3p and circ_0011292 or CHEK1. Xenograft tumor model was constructed for determining the effect of circ_0011292 in NSCLC growth in vivo.

Results: Circ_0011292 was upregulated in PTX-resistant NSCLC tissues and cells. Circ_0011292 or CHEK1 knockdown enhanced PTX sensitivity and cell apoptosis, and repressed cell proliferation, migration, and invasion in PTX-resistant NSCLC cells. Mechanistically, circ_0011292 was a sponge of miR-433-3p and miR-433-3p directly targeted CHEK1. Meanwhile, silencing miR-433-3p or overexpressing CHEK1 respectively abrogated the impacts of circ_0011292 deletion or miR-433-3p introduction on PTX resistance and cell progression in PTX-resistant NSCLC cells in vitro. Moreover, circ_0011292 could positively modulate CHEK1 expression through sponging miR-433-3p. In addition, circ_0011292 knockdown retarded tumor growth of NSCLC in vivo.

Conclusion: Circ_0011292 could accelerate PTX resistance and cell malignant progression of NSCLC cells partially through the regulation of circ_0011292/miR-433-3p/CHEK1 axis.

Abbreviations: NSCLC, non-small-cell lung cancer; PTX, paclitaxel; qRT-PCR, quantitative real-time polymerase chain reaction; CHEK1, checkpoint kinase 1; CCK-8, Cell Counting Kit-8; GAPDH, glyceraldehyde-phosphate dehydrogenase; RNase, Ribonuclease; FITC, fluorescein isothiocyanate; PI, propidium iodide; SDS-PAGE, sodium dodecyl sulfate-polyacrylamide gel; MMP9, matrix metalloproteinase 9; ANOVA, analysis of variance.

Ming Jin and Fengping Zhang contributed equally to this paper.

This is an open access article under the terms of the [Creative Commons Attribution-NonCommercial-NoDerivs](https://creativecommons.org/licenses/by-nc-nd/4.0/) License, which permits use and distribution in any medium, provided the original work is properly cited, the use is non-commercial and no modifications or adaptations are made.

© 2022 The Authors. *Thoracic Cancer* published by China Lung Oncology Group and John Wiley & Sons Australia, Ltd.

KEYWORDS

CHEK1, circ_0011292, miR-433-3p, NSCLC, PTX

BACKGROUND

Lung cancer is the most prevalent malignancy leading to cancer death globally, with non-small-cell lung cancer (NSCLC) accounting for approximately 85% of lung cancer cases.^{1,2} Chemoresistance has been a major challenge in the clinical treatment of cancer.³ Paclitaxel (PTX), an antineoplastic drug for NSCLC, becomes less effective overtime due to the acquisition of chemoresistance.⁴ Hence, there is an urgent need to elucidate the molecular basis of tumorigenesis and PTX resistance of NSCLC for developing effective therapeutic interventions.

Circular RNAs (circRNAs) are endogenous non-coding RNAs (ncRNAs) possessing high stabilization due to their covalently closed-loop structures.⁵ CircRNAs have been identified as pivotal participators in the drug resistance and carcinogenesis of multifarious cancers, including NSCLC.^{6,7} For example, circ-PRMT5 was discovered to facilitate cisplatin resistance through regulating miR-4458/REV3L axis in NSCLC.⁸ Circ_0002483 could restrain NSCLC malignant behaviors and increase PTX sensitivity in NSCLC by sponging miR-182-5p.⁹ Furthermore, Guo et al. uncovered that circ_0011292 was overexpressed in NSCLC and functioned as a potential promoter in the tumorigenesis and PTX resistance of NSCLC by regulating the miR-379-5p/TRIM65 axis.¹⁰ Nonetheless, the detailed action played by circ_0011292 in carcinogenesis and PTX resistance in NSCLC is still not fully disclosed.

MicroRNAs (miRNAs) are small ncRNAs which can modulate tumor process through the interaction with the 3'-untranslated regions (3'-UTRs) of target mRNAs.^{11,12} Emerging evidence has demonstrated that many miRNAs are implicated in the development and PTX resistance of NSCLC. For instance, miR-4262 could sensitize NSCLC cells to PTX via the inhibition of PTEN¹³ and miR-30a-5p could reduce the PTX resistance of NSCLC cells by targeting BCL-2.¹⁴ Previous studies have confirmed that miR-433-3p was lowly expressed and its overexpression impeded cell growth via upregulating WT1 associated protein in NSCLC.¹⁵ Moreover, checkpoint kinase 1 (CHEK1) is also known as CHK1 and activated to phosphorylate key regulators related to cell proliferation, capoptosis, and DNA repair.¹⁶ CHEK1 was elevated in NSCLC and its inhibition enhanced the sensitivity of NSCLC cells to pemetrexed.¹⁷ However, the role of miR-433-3p and its correlation with CHEK1 in the modulation of PTX resistance of NSCLC cells remains unclear.

In this current study, we mainly investigated the biological role of circ_0011292 in the progression of PTX-resistant NSCLC cells. Meanwhile, circ_0011292 might serve as a competing endogenous RNA (ceRNA) of miR-433-3p to influence CHEK1 expression, thereby regulating NSCLC cell malignant behaviors in vitro and in vivo. Thus, we further elucidated the novel circRNA/miRNA/mRNA signal mechanism based on circ_0011292 in NSCLC during this study.

METHODS

Clinical specimens

Forty-one pairs of NSCLC tissue specimens and adjacent noncancerous tissue specimens were harvested from NSCLC patients through surgical resection at Jingmen No.1 People's Hospital. The obtained clinical tissues were maintained at -80°C until use. All participators did not receive any other radiotherapy, chemotherapy or related therapies before study initiation. This study was approved by the Ethics Committee of Jingmen No.1 People's Hospital and implemented in keeping with the Declaration of Helsinki. Written informed consent was received from each patient.

Cell culture

Human normal lung fibroblast cell line (MRC-5) and NSCLC cell lines (A549 and H1299) were received from the American Type Culture Collection (Rockville, MD, USA). All cells were cultivated in RPMI-1640 medium (Invitrogen) plus 10% fetal bovine serum (FBS; Invitrogen) and 1% penicillin/streptomycin (Invitrogen) in a humidified air atmosphere with 5% CO_2 at 37°C . To establish PTX-resistant NSCLC cells (A549/PTX and H1299/PTX), A549 and H1299 cells were exposed to escalating concentrations of paclitaxel (PTX) (Solarbio). An additional 5 nM PTX (Solarbio) was added in the culture media to maintain the resistant phenotype.

Cell transfection

For the knockdown of circ_0011292 or CHEK1, small interfering RNA (siRNA) targeting circ_0011292 (si-circ_0011292#1 and si-circ_0011292#2) or CHEK1 (si-CHEK1) was severally constructed, with scrambled siRNA (si-NC) served as negative control. For miR-433-3p overexpression or knockdown, the miR-433-3p mimic (miR-433-3p) or inhibitor (in-miR-433-3p) was separately generated, with miR-NC or in-miR-NC acted as negative control. The sequence of CHEK1 was amplified by PCR and cloned into pcDNA3.1 plasmid (vector; Invitrogen) to create CHEK1 overexpression plasmid (CHEK1), with non-target plasmid (vector) as the negative control. For circ_0011292 stable knockdown, lentiviral vectors carrying circ_0011292 short hairpin RNA (sh-circ_0011292) or negative control (sh-NC) were also established. Then, the synthetic oligonucleotides or vectors synthesized from Ribobio were transfected into PTX-resistant NSCLC cells utilizing Lipofectamine 3000 (Invitrogen). Forty-eight hours post-transfection, cells were harvested for further analysis.

Quantitative real-time polymerase chain reaction

Total RNA was extracted from tissues and cells utilizing RNAiso Plus (Takara). The RNA was transcribed into cDNA utilizing One Step TB Green[®] PrimeScript[™] PLUS RT-PCR Kit (Takara) or miScript Reverse Transcription Kit (Qiagen). Then, the quantitative real-time polymerase chain (qRT-PCR) reaction was manipulated using SYBR Premix Ex Taq[™] kit (Takara) and specific primers (Sangon) on a 7500 Real-Time PCR system (Applied Biosystems). The relative expression was analyzed using the $2^{-\Delta\Delta Ct}$ method (Ct, cycle threshold) and normalized based on the expression of internal controls U6 (for miRNA) or glyceraldehyde-phosphate dehydrogenase (GAPDH) (for circRNA and mRNA). The primer sequence was listed as follows: circ_0011292: (F: 5'-A CATCTACCAGGTCCTCTGT-3' and R: 5'-ATGG TTCTTGGTCACTGCGCA-3'); Tubulointerstitial nephritis antigen-like 1 (TINAGL1): (F: 5'-ACCAGGTCCTCTGT TCTACC-3' and R: 5'-TGCCTCCCTTGTATAGGAAG AA-3'); miR-433-3p: (F: 5'-TGATGGGCTCCTCGGT-3' and R: 5'-GAACATGTCTGCGTATCTC-3'); CHEK1: (F: 5'-TT CCATCAACTCATGGCAGG-3' and R: 5'-ACGCTCACGA TTATTATACCGAA-3'); GAPDH: (F: 5'-GACCACAGTCCA TGCCATCAC-3' and R: 5'-ACGCCTGCTTACCACCTT -3'); U6: (F: 5'-CTCGCTTCGGCAGCACA-3' and R: 5'-AACGCTTACGAATTTGCGT-3').

Ribonuclease R digestion

To assess the stability of circ_0011292, Ribonuclease (RNase) R (Epicenter Technologies) was utilized to digest linear RNA. In brief, total RNA (2 μ g) was incubated for 20 min with or without RNase R (3 U/ μ g) at 37°C. After that, the treated RNA was used for qRT-PCR to examine the expression of circ_0011292 and linear isoform TINAGL1.

Cell Counting Kit-8 assay

Cell Counting Kit-8 (CCK-8) assay was employed to determine the half maximal inhibitory concentration (IC50) value of PTX and cell viability. For PTX resistance measurement, transfected cells (1×10^4 cells/well) were seeded in 96-well plates and cultivated overnight, and then different doses of PTX (0.05, 0.2, 0.8, 3.2, 12.8 μ M) were individually added into the well prior to cell viability analysis. For cell viability detection, transfected cells were plated in 96-well plates at 5×10^3 per well. After culture for 48 h, 10 μ L CCK-8 solution (5 mg/mL; Beyotime) was pipetted into each well for another 4 h of incubation at 37°C. Finally, the optical density (OD) value at 450 nm was measured with a microplate reader (BioTek) for assessing cell viability and the IC50.

5-ethynyl-2'-deoxyuridine incorporation assay

Cell-Light EDU Apollo 567 In Vitro Imaging Kit (Ribobio) was utilized to inspect the proliferation capacities of A549/PTX and H1299/PTX cells through assessing DNA synthetic ability. Briefly, transfected cells were trained for 48 h in 96-well plates at 37°C. Then, cells were immobilized by paraformaldehyde (4%; Beyotime) and permeabilized with Triton X-100 (0.5%; Solarbio) for 10 min in indoor environment. Later, cells were added to 10 μ M 5-ethynyl-2'-deoxyuridine (Edu) for 2 h-incubation at 37°C, and 5 μ g/mL DAPI solution (Solarbio) was used to stain cell nuclei for 10 min. Finally, the number of Edu-positive cells was counted under a fluorescence microscope (100 \times ; Olympus) in five randomly selected areas.

Colony formation assay

Transfected A549/PTX and H1299/PTX cells were planted in 24-well plates in maintenance medium, followed by cultivation for 2 weeks. After being immobilized with ethanol (70%) and dyed with crystal violet (0.1%; Beyotime), the formed colonies (>50 cells) were counted using a microscope (Olympus).

Flow cytometry analysis

For cycle distribution detection, transduced A549/PTX and H1299/PTX cells were gathered and re-suspended in PBS following 48 h of transfection. After RNase treatment, A549/PTX and H1299/PTX cells were immobilized with 70% ethanol followed by the incubation of propidium iodide (PI; Solarbio) at 37°C for 30 min. Then, the cycle distribution of A549/PTX and H1299/PTX cells at different phases was examined by flow cytometry (BD Biosciences).

Annexin V-fluorescein isothiocyanate (FITC) Apoptosis Detection Kit (Vazyme) was utilized for detecting cell apoptosis. After different transfection for 48 h, A549/PTX and H1299/PTX cells were harvested and double-stained with 5 μ L of FITC-labeled Annexin V and 5 μ L of PI. The apoptotic cells were measured utilizing flow cytometry (BD Biosciences).

Transwell assay

Transfected A549/PTX and H1299/PTX cells were collected to measure the abilities of migration and invasion using transwell chambers (Corning). For cell migration analysis, transfected cells (2×10^4) in serum-free media plus 5 nM PTX were plated on the upper chamber, then 500 μ L of culture medium containing 10% FBS was added to the lower chamber. This transwell system was cultivated in normal cell culture conditions for another 24 h. Next, the migrated cells

on the bottom of chamber were fixed with 4% paraformaldehyde (Beyotime) for 30 min and stained with 0.1% crystal violet (Beyotime) for 30 min. The images of cells were captured under a microscope (100 \times ; Olympus) and the migrated cell number was calculated according to five randomly selected fields. For cell invasion analysis, transwell chambers were pre-coated with Matrigel (BD Biosciences), and 2×10^5 cells were used; the other procedures were the same as for the migration assay.

Western blot assay

Protein extraction was implemented utilizing RIPA Lysis Buffer (Beyotime). The concentrations of protein samples were examined with a BCA protein assay kit (Tiangen). After separation by 10% sodium dodecyl sulfonate-polyacrylamide gel (SDS-PAGE; Solarbio) electrophoresis, the protein sample (20 μ g) was blotted onto polyvinylidene difluoride membrane (Corning) and then blocked with 5% non-fat milk (Solarbio) for 1 h. Afterwards, the membranes were immunoblotted with primary antibodies against CHEK1 (1:10000, ab32531; Abcam), proliferating cell nuclear antigen (PCNA) (1:2000, ab152112; Abcam), Ki67 (1:1000, ab243878; Abcam), matrix metalloproteinase 9 (MMP9) (1:1000, ab38898; Abcam), Bcl-2-associated X protein (Bax, 1:1000, ab53154; Abcam) and GAPDH (1:10000, ab181602; Abcam) overnight at 4°C followed by interaction with Goat Anti-Rabbit IgG H&L (HRP) secondary antibody (1:10000, ab205718; Abcam) for 2 h at indoor temperature. Finally, the intensity of protein bands was assessed utilizing BeyoECL Plus ECL Kit (Beyotime).

Dual-luciferase reporter assay

The sequences of circ_0011292 and the 3'-UTR of CHEK1 containing the putative miR-433-3p binding sites or mutant binding sites were individually inserted into pmirGLO vectors (Promega) to generate the luciferase reporter vectors, named as wt-circ_0011292, mut-circ_0011292, wt-CHEK1 3'UTR, and mut-CHEK1 3'UTR, respectively. A549 and H1299 cells (1×10^5 cells per well) were seeded into 24-well plates and then transfected with the above-generated reporters together with miR-433-3p or negative control miR-NC for 48 h using Lipofectamine 3000 reagent (Invitrogen). The luciferase activity was determined using a Dual-Luciferase Reporter Assay System (Promega).

Xenograft tumor models

The xenograft experiment was performed in 6-week-old male BALB/c nude mice (Beijing Vital River Laboratory Animal Technology Co., Ltd). The mice were divided into two groups ($n = 6$ /group): sh-circ_0011292 and sh-NC. A549/PTX cells (5×10^6 cells) stably transfected with sh-NC or sh-circ_0011292 were subcutaneously implanted into the right

back of nude mice. After inoculation, tumor volume was calculated every 7 days using the formula: $0.5 \times \text{length} \times \text{width}^2$. Twenty-eight days later, the mice were euthanized and neoplasms were resected and weighted. The animal experiments were allowed by the Ethics Committee of Animal Research of Jingmen No.1 People's Hospital.

Statistical analysis

The experiments were conducted with at least three separate assays, and the resulting data are presented as mean \pm standard deviation following analyzed by GraphPad Prism Version 7.0 Software (GraphPad). Difference analysis was executed with Student's *t*-test or one-way analysis of variance (ANOVA) followed by Tukey's post hoc test. $p < 0.05$ was defined as statistically significant.

RESULTS

Circ_0011292 and CHEK1 were highly expressed in NSCLC tissues and PTX-resistant cells

To elucidate the function of circ_0011292 in NSCLC, qRT-PCR assay was first performed to examine the expression pattern of circ_0011292 in NSCLC cancer tissues (Cancer) and adjacent normal tissues (Normal). The results showed that circ_0011292 in NSCLC tissues was highly expressed relative to that in matched normal tissues (Figure 1a). Meanwhile, circ_0011292 was upregulated in NSCLC cell lines (A549 and H1299) versus normal MRC-5 cell line, and it was even higher in PTX-resistant NSCLC cell lines (A549/PTX and H1299/PTX) than parental cell lines (Figure 1b). Like the expression of circ_0011292, the mRNA and protein levels of CHEK1 were also elevated in NSCLC tissues compared to that in adjacent normal tissues (Figure 1c,d). In parallel, CHEK1 mRNA and protein expression was dramatically raised in A549 and H1299 cells in contrast to MRC-5 cells, and it was further enhanced in A549/PTX and H1299/PTX cells relative to that in their parents (Figure 1e,f). These outcomes indicate that circ_0011292 and CHEK1 might play a vital role in the regulation of PTX resistance in NSCLC cells.

Circ_0011292 silence inhibited PTX resistance, proliferation, migration, invasion, and enhanced apoptosis in PTX-resistant NSCLC cells

Next, the stability of circ_0011292 in A549/PTX and H1299/PTX cells was identified by RNase R digestion assay. The qRT-PCR result suggested that circ_0011292 was resistant to RNase R compared with its linear isoform TINAGL1 in A549/PTX and H1299/PTX cells (Figure 2a). To investigate the biological effect of circ_0011292 on the malignant

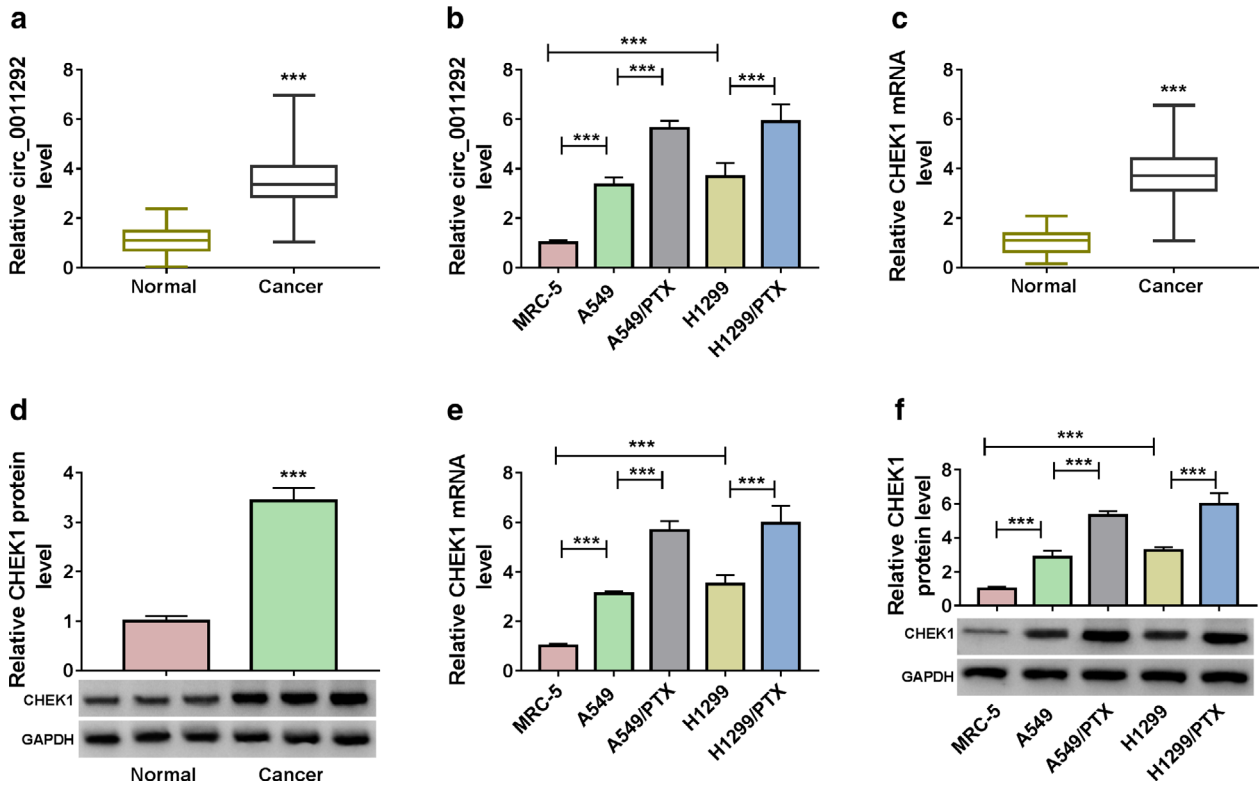


FIGURE 1 Circ_0011292 and CHEK1 were overexpressed in NSCLC tissues and PTX-resistant cells. (a) The expression of circ_0011292 in NSCLC cancer tissues (Cancer) and adjacent normal tissues (Normal) was detected by qRT-PCR assay. (b) qRT-PCR assay was conducted for the level of circ_0011292 in normal MRC-5 cell line, PTX-resistant NSCLC cell lines (A549/PTX and H1299/PTX), and parental cell lines (A549 and H1299). (c and d) The mRNA and protein levels of CHEK1 in NSCLC cancer tissues (Cancer) and adjacent normal tissues (Normal) were measured using qRT-PCR assay and western blot assay, respectively. (e and f) The mRNA and protein expression of CHEK1 in MRC-5, A549, H1299, A549/PTX, and H1299/PTX cells was also measured using qRT-PCR assay and western blot assay, respectively. *** $p < 0.001$

behaviors of PTX-resistant NSCLC cells, loss-of-function experiments were conducted by silencing the expression of circ_0011292 using siRNA transfection. As displayed in Figure 2b, circ_0011292 was distinctly downregulated following the transfection of si-circ_0011292#1 or si-circ_0011292#2 in A549/PTX and H1299/PTX cells relative to si-NC control, indicating the successful transfection of circ_0011292. For the higher transfection efficiency of si-circ_0011292#1, it was selected for subsequent assays. By contrast, the IC₅₀ value of PTX and cell viability in PTX-resistant A549/PTX and H1299/PTX cells were significantly increased than their parental cells (Figure 2c,d), suggesting an acquired PTX resistance in A549/PTX and H1299/PTX cells. CCK-8 assay also revealed that si-circ_0011292#1 transfection led to a significant decrease in the IC₅₀ value of PTX in A549/PTX and H1299/PTX cells (Figure 2e), implying that circ_0011292 knockdown suppressed the resistance of A549/PTX and H1299/PTX cells to PTX. Edu incorporation assay showed that the ratio of Edu-positive cells in A549/PTX and H1299/PTX cells transfected with si-circ_0011292#1 was distinctly decreased (Figure 2f). Colony formation assay indicated that the colony forming ability of A549/PTX and H1299/PTX cells was blocked by circ_0011292 silence (Figure 2g). Flow cytometry analysis suggested that knockdown of circ_0011292 markedly

induced cell cycle arrest at G₀/G₁ phase (Figure 2h,i). Meanwhile, the protein expression of proliferation-related makers (PCNA and Ki67) was dramatically reduced in A549/PTX and H1299/PTX cells after si-circ_0011292#1 introduction (Figure 2j). Furthermore, transwell assay exhibited that the numbers of migrated and invaded cells were reduced in A549/PTX and H1299/PTX cells due to circ_0011292 deficiency (Figure 2k,l). The apoptosis rate of A549/PTX and H1299/PTX cells was visibly increased after transfection with si-circ_0011292#1 (Figure 2m). Additionally, western blot data showed that circ_0011292 silence suppressed the expression of metastasis-associated protein MMP9 and promoted the expression of pro-apoptotic protein Bax in the two PTX-resistant NSCLC cells (Figure 2n). These data demonstrate that circ_0011292 knockdown has a suppressive role in PTX resistance and the progression of PTX-resistant NSCLC cells in vitro.

Circ_0011292 functioned as a sponge of miR-433-3p and miR-433-3p directly interacted with CHEK1

The circRNA/miRNA/mRNA regulatory network has been identified in the progression of multifarious cancers.^{18,19} To

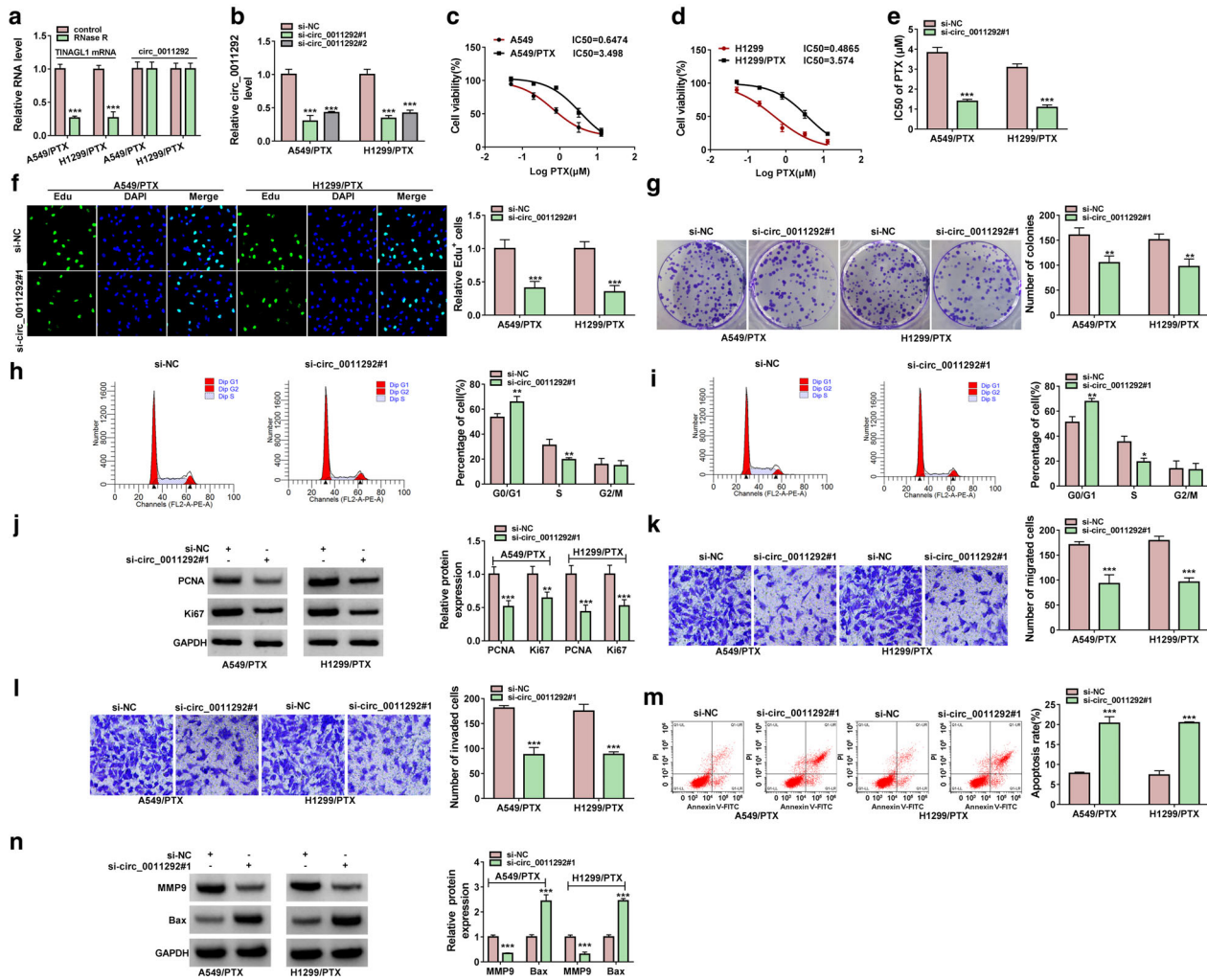


FIGURE 2 Circ_0011292 knockdown hindered PTX resistance, proliferation, migration, invasion, and accelerated apoptosis in PTX-resistant NSCLC cells. (a) qRT-PCR assay was performed to determine the RNA level of circ_0011292 and linear TINAGL1 after RNase R treatment or not in PTX-resistant NSCLC cells. (b) The expression of circ_0011292 in A549/PTX and H1299/PTX cells transfected with si-circ_0011292#1, si-circ_0011292#2 or si-NC was determined using qRT-PCR assay. (c and d) The cell viability and IC50 value of PTX in A549, H1299, A549/PTX, and H1299/PTX cells were tested by CCK-8 assay. (E-N) A549/PTX and H1299/PTX cells were transfected with si-circ_0011292#1 or si-NC. (E) CCK-8 assay identified IC50 value of PTX in transfected cells. (f) Edu incorporation assay was implemented for the ratio of Edu-positive cells. Cell proliferation rate = (Edu-positive cells)/(total number of cells) \times 100%. (g) Colony formation ability was tested by colony formation assay. (h and i) Cell cycle was monitored via flow cytometry. (j) The protein expression of PCNA and Ki67 was measured by western blot. (k and l) Transwell assay measured the numbers of migrated cells and invaded cells in PTX-resistant NSCLC cells after transfection. (m) The apoptosis rate in transfected cells was analyzed by flow cytometry. (n) The levels of metastasis-associated protein MMP9 and pro-apoptotic proteins Bax in transfected cells were measured through western blot assay. * $p < 0.05$, ** $p < 0.01$, and *** $p < 0.001$

further understand the role of circ_0011292 in NSCLC, the potential miRNAs pairing to circ_0011292 and CHEK1 was explored. The CircInteractome (<https://circinteractome.nia.nih.gov/>) online tool predicted that circ_0011292 harbored putative complementary binding sites with miR-433-3p (Figure 3a). Interestingly, CHEK1 was predicted to be a target gene of miR-433-3p using online tool starBase 3.0 (<http://starbase.sysu.edu.cn/>) (Figure 3c). The interaction relationships between miR-433-3p and circ_0011292 or CHEK1 were validated by dual-luciferase reporter assay. The results revealed that transient transfection of wild-type circ_0011292 or CHEK1 3'-UTR reporter (wt-circ_0011292 or wt-CHEK1 3'-UTR) in the presence of miR-433-3p mimic caused a remarkable suppression of luciferase activity in A549 and H1299 cells,

and this effect was completely abolished by the mutation of the miR-433-3p-pairing sequence (mut-circ_0011292 or mut-CHEK1 3'-UTR) (Figure 3b,d), suggesting a combination between miR-433-3p and circ_0011292 or CHEK1. Subsequently, qRT-PCR data revealed that miR-433-3p was down-regulated in NSCLC tissues and cells when compared to the normal controls, and there was a more prominent decrease of miR-433-3p in PTX-resistant NSCLC counterparts (A549/PTX and H1299/PTX) relative to parental cells (Figure 3e,f). Moreover, circ_0011292 interference led to an enhanced level of miR-433-3p (Figure 3g) and reduced protein level of CHEK1 (Figure 3h) in A549/PTX and H1299/PTX cells. Additionally, the regulation of miR-433-3p on the expression of CHEK1 was determined. The overexpression or

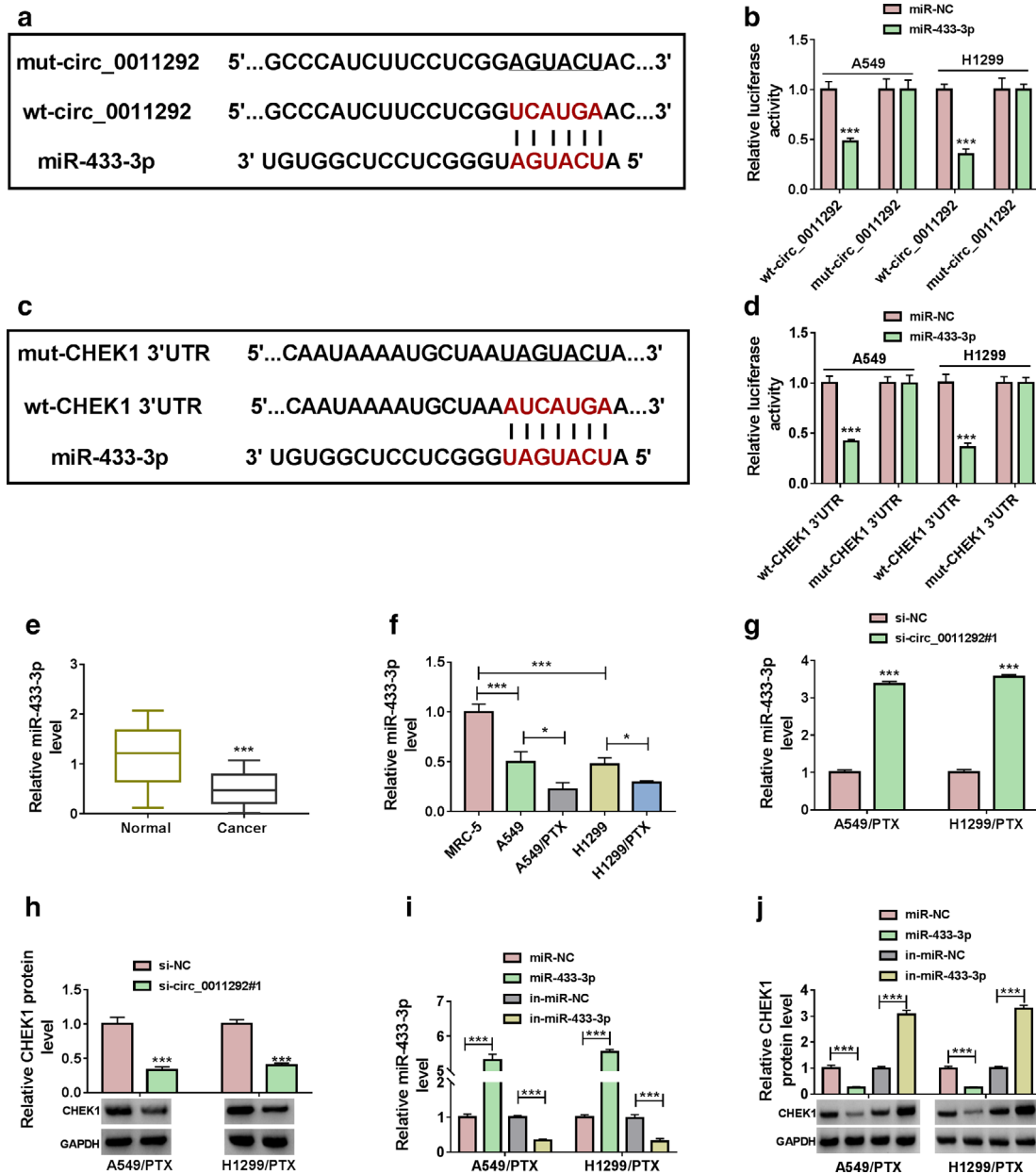


FIGURE 3 Circ_0011292 sponged miR-433-3p and CHEK1 was directly targeted by miR-433-3p. (a) The complementary sequence between miR-433-3p and circ_0011292 was presented. (b) The luciferase activity in A549 and H1299 cells co-transfected with miR-433-3p or miR-NC and wt-circ_0011292 or mut-circ_0011292 was measured by dual-luciferase reporter assay. (c) The potential binding sites between CHEK1 3'UTR and miR-433-3p were predicted by starBase 3.0. (d) The combination between miR-433-3p and CHEK1 was demonstrated by dual-luciferase reporter assay. (e) The expression of miR-433-3p in NSCLC cancer tissues (Cancer) and adjacent normal tissues (Normal) was tested by qRT-PCR assay. (f) The level of miR-433-3p in MRC-5, A549, H1299, A549/PTX, and H1299/PTX cells was examined via qRT-PCR assay. (g and h) The levels of miR-433-3p and CHEK1 in A549/PTX and H1299/PTX cells transfected with si-circ_0011292#1 or si-NC were measured via qRT-PCR assay and western blot assay, respectively. (i and j) The abundances of miR-433-3p and CHEK1 in A549/PTX and H1299/PTX cells after miR-433-3p overexpression or knockdown were determined via qRT-PCR and western blot assays, respectively. * $p < 0.05$, and *** $p < 0.001$

knockdown transfection efficiency of miR-433-3p mimic and inhibitor (miR-433-3p and in-miR-433-3p) was examined by qRT-PCR (Figure 3i). Western blot data revealed that the transfection of miR-433-3p mimic resulted in decreased CHEK1 expression, while the transfection of in-miR-433-3p remarkably promoted CHEK1 expression (Figure 3j). These results show a direct interaction between miR-433-3p and circ_0011292 or CHEK1 in NSCLC cells.

CHEK1 knockdown restrained PTX resistance and the malignant behaviors of PTX-resistant NSCLC cells

To validate the precise role of CHEK1 in PTX resistance of NSCLC cells, si-CHEK1 was transfected into A549/PTX and H1299/PTX cells. The mRNA and protein expression levels of CHEK1 were obviously reduced in

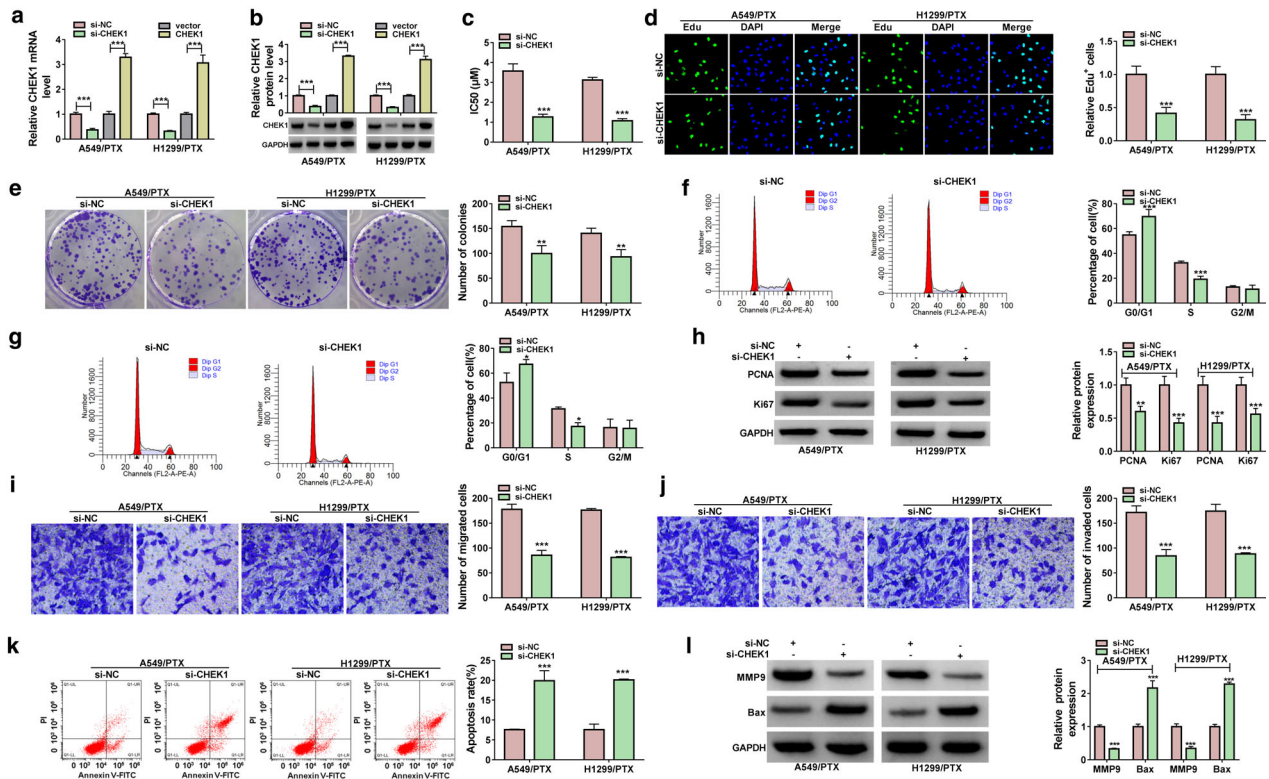


FIGURE 4 CHEK1 knockdown contributed to PTX sensitivity and blocked cell malignant behaviors in PTX-resistant NSCLC cells. A549/PTX and H1299/PTX cells were transfected with si-CHEK1 or si-NC. (a and b) The mRNA and protein expression of CHEK1 in A549/PTX and H1299/PTX cells were assessed using qRT-PCR and Western blot assays, respectively. (c) The IC₅₀ of PTX in transfected cells was measured by CCK-8 assay. (d and e) Cell proliferation was assessed using Edu incorporation assay (d) and colony formation assay (e). (f and g) Flow cytometry was conducted for cell cycle distribution. (h) Western blot was employed for the protein expression of PCNA and Ki67. (i and j) Cell migration and invasion were examined by transwell assay in transfected cells. (k) Cell apoptosis was evaluated by flow cytometry. (l) Western blot assay was implemented to inspect MMP9 and Bax protein levels. * $p < 0.05$, ** $p < 0.01$, and *** $p < 0.001$

A549/PTX and H1299/PTX cells after CHEK1 knockdown, while they were dramatically increased after CHEK1 overexpression (Figure 4a,b). This result showed that A549/PTX and H1299/PTX cells were successfully transfected with CHEK1 and si-CHEK1. Meanwhile, CHEK1 knockdown notably repressed the resistance of A549/PTX and H1299/PTX cells to PTX compared to control group, as demonstrated by the decreased IC₅₀ value of PTX following CHEK1 downregulation (Figure 4c). Functional analyses data revealed that CHEK1 deficiency caused an apparent inhibition in proliferation (Figure 4d), colony formation (Figure 4e), cell cycle progression (Figure 4f,g), PCNA and Ki67 expression (Figure 4h), migration (Figure 4i), and invasion (Figure 4j) and an obvious enhancement in cell apoptosis (Figure 4k) in A549/PTX and H1299/PTX cells. In addition, the protein level of MMP9 was decreased and the protein level of Bax was increased in A549/PTX and H1299/PTX cells after CHEK1 silence (Figure 4l). Collectively, these findings attested that CHEK1 knockdown repressed PTX resistance and cell progression in PTX-resistant NSCLC cells.

Inhibition of miR-433-3p reversed the impacts mediated by circ_0011292 deficiency on the malignant development of PTX-resistant NSCLC cells

To further investigate whether circ_0011292 regulated PTX resistance and cell behaviors in PTX-resistant NSCLC cells by targeting miR-433-3p, rescue experiments were carried out by transfecting si-NC, si-circ_0011292#1, si-circ_0011292#1 + in-miR-NC or si-circ_0011292#1 + in-miR-433-3p into A549/PTX and H1299/PTX cells. The qRT-PCR result showed that si-circ_0011292#1-induced enhanced impact on the expression of miR-433-3p was effectively overturned by miR-433-3p silence (Figure 5a). Furthermore, circ_0011292 deletion-induced inhibition on IC₅₀ of PTX (Figure 5b), proliferation (Figure 5c), colony formation (Figure 5d), cell cycle progression (Figure 5e,f), PCNA and Ki67 expression (Figure 5g), migration (Figure 5h), and invasion (Figure 5i) were attenuated by miR-433-3p downregulation in A549/PTX and H1299/PTX cells. Cell apoptosis was overtly enhanced in circ_0011292-silenced A549/PTX and H1299/PTX cells, and this promotion was repressed by in-miR-433-3p introduction (Figure 5j). In addition, the effect of circ_0011292

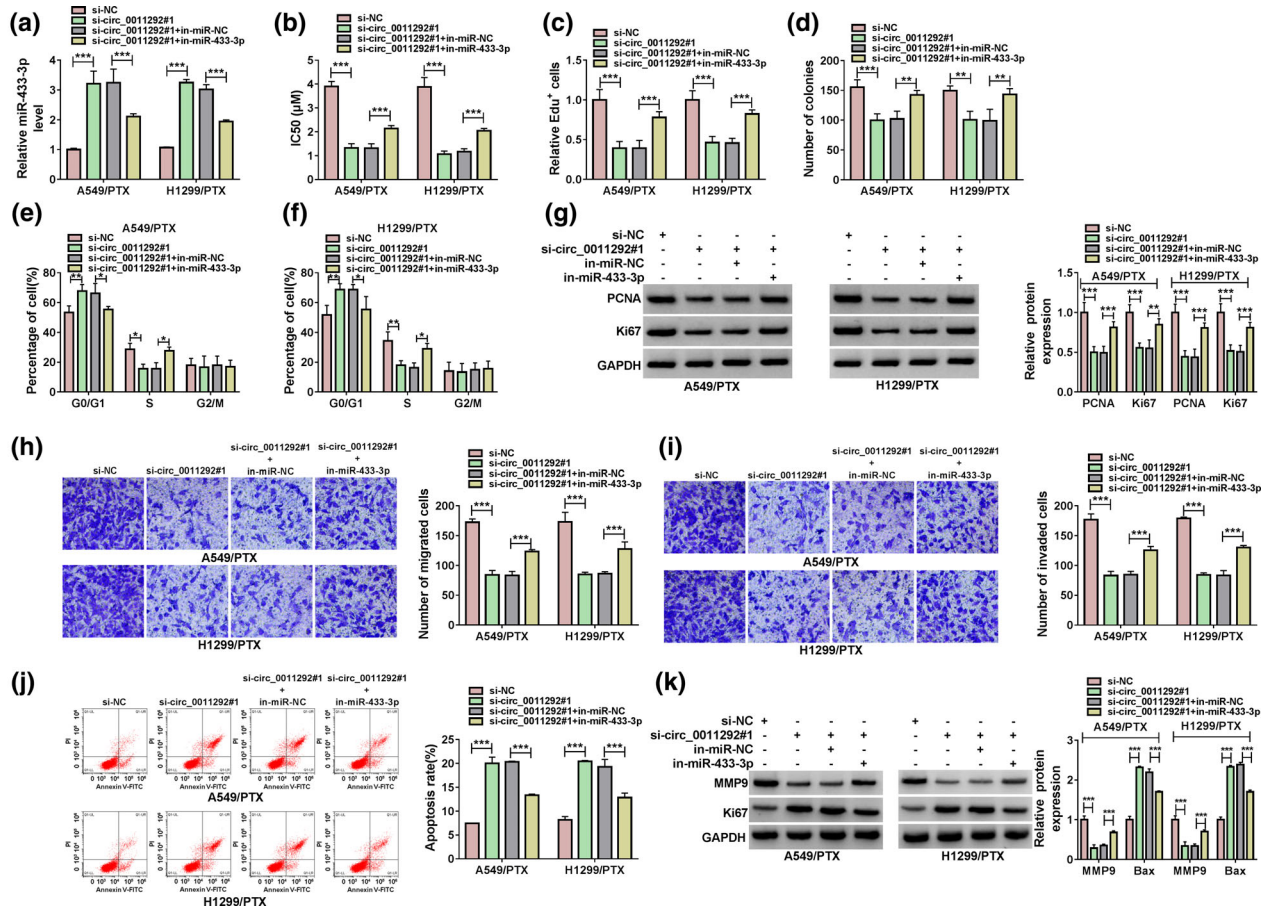


FIGURE 5 The regulatory impacts of circ_0011292#1 silence on PTX-resistant NSCLC cell behaviors were abated by miR-433-3p downregulation. A549/PTX and H1299/PTX cells were transfected with si-NC, si-circ_0011292#1, si-circ_0011292#1 + in-miR-NC or si-circ_0011292#1 + in-miR-433-3p. (a) qRT-PCR detected the miR-433-3p level in transfected A549/PTX and H1299/PTX cells. (b–j) The IC₅₀ of PTX, the ratio of Edu-positive cells, the number of colonies, cell cycle distribution, PCNA and Ki67 expression, cell migration, and invasion, as well as cell apoptosis in transfected cells were severally measured by CCK-8 assay, Edu incorporation assay, colony formation assay, western blot assay, transwell assay or flow cytometry analysis. (k) The protein levels of MMP9 and Bax in transfected cells were measured through western blot assay. * $p < 0.05$, ** $p < 0.01$, and *** $p < 0.001$

knockdown on the expression of MMP9 and Bax was rescued by the presence of in-miR-433-3p (Figure 5k). Taken together, these findings suggested that circ_0011292#1 deficiency exerted a suppressive effect on PTX resistance and cell progression in PTX-resistant NSCLC cells by upregulating miR-433-3p expression.

CHEK1 overexpression could reverse miR-433-3p-mediated effects on PTX resistance and cell malignant behaviors in PTX-resistant NSCLC cells

Next, the effects of miR-433-3p and CHEK1 on PTX resistance and cell development in PTX-resistant NSCLC cells were further determined. A549/PTX and H1299/PTX cells were transfected with miR-NC, miR-433-3p, miR-433-3p + vector or miR-433-3p + CHEK1. As observed in Figure 6a,b, miR-433-3p mimic transfection evidently decreased the mRNA and protein levels of CHEK1 in both A549/PTX and H1299/PTX cells, whereas CHEK1

overexpression partially reversed the effects, hinting at the high transfection efficiency of them. By contrast, the increased miR-433-3p expression led to a noteworthy reduction in IC₅₀ value of PTX (Figure 6c) and a significant suppression in the ratio of Edu positive cells (Figure 6d), colony formation (Figure 6e), cell cycle progression (Figure 6f,g), PCNA and Ki67 expression (Figure 6h), migration (Figure 6i), and invasion (Figure 6j), as well as a remarkable promotion in cell apoptosis (Figure 6k) in both Huh7-R and SNU-387-R cells. In addition, miR-433-3p upregulation caused a prominent decrease in the level of MMP9 and a remarkable increase in the level of Bax in A549/PTX and H1299/PTX cells (Figure 6l). Nevertheless, these impacts of miR-433-3p overexpression in both A549/PTX and H1299/PTX cells were effectively attenuated by enhancing CHEK1 expression (Figure 6c–l). These results collectively demonstrate that miR-433-3p overexpression represses PTX resistance and cell malignant behaviors in PTX-resistant NSCLC cells by targeting CHEK1.

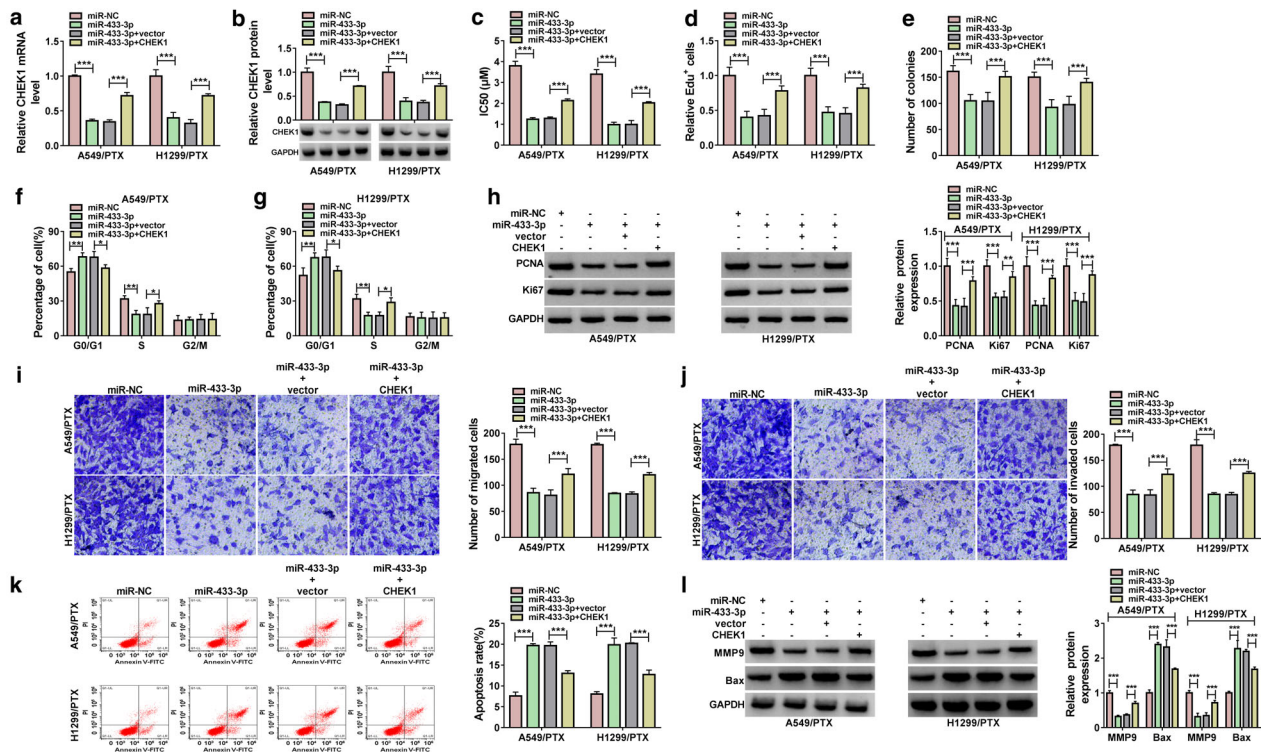


FIGURE 6 MiR-433-3p overexpression contributed to PTX sensitivity and suppressed cell progression in PTX-resistant NSCLC cells by interacting with CHEK1. A549/PTX and H1299/PTX cells were transfected with miR-NC, miR-433-3p, miR-433-3p + vector or miR-433-3p + CHEK1. (a and b) The mRNA and protein levels of CHEK1 in A549/PTX and H1299/PTX cells after transfection were detected using qRT-PCR assay and Western blot assay, respectively. (c) The IC₅₀ value of PTX in transfected cells were assessed by CCK-8 assay. The ratio of Edu-positive cells (d), colony formation numbers (e), cell cycle distribution (f and g), PCNA, and Ki67 expression (h) were examined via Edu incorporation assay, colony formation assay, flow cytometry, and western blot assay, respectively. (i and j) Cell migration and invasion capacities were inspected by transwell assay. (k) Cell apoptosis was analyzed by flow cytometry. (l) Western blot assay was utilized for the protein levels of MMP9 and Bax in transfected A549/PTX and H1299/PTX cells. **p* < 0.05, ***p* < 0.01, and ****p* < 0.001

Knockdown of circ_0011292 restrained tumor growth of NSCLC cells via circ_0011292/ miR-433-3p/CHEK1 axis in vivo

To further analyze the relationships among circ_0011292, miR-433-3p, and CHEK1 in PTX-resistant NSCLC cells, A549/PTX and H1299/PTX cells were transfected with si-NC, si-circ_0011292#1, si-circ_0011292#1 + in-miR-NC or si-circ_0011292#1 + in-miR-433-3p for the detection of CHEK1 mRNA and protein expression. As expected, in comparison with their counterparts, the transfection of si-circ_0011292#1 led to a conspicuous reduction of CHEK1 mRNA and protein levels in both A549/PTX and H1299/PTX cells, while these effects were remarkably relieved by miR-433-3p inhibitor (Figure 7a,b). These outcomes suggested that circ_0011292 positively regulated CHEK1 expression through working as a sponge of miR-433-3p in PTX-resistant NSCLC cells.

Finally, the effect of circ_0011292 on NSCLC tumor growth in vivo was explored by constructing a xenograft tumor mice model. A549/PTX cells stably transfected with sh-circ_0011292 or sh-NC were implanted into the nude mice. As shown in Figure 7c,d, the volume and weight of xenograft tumors were evidently reduced by

sh-circ_0011292 transfection. The qRT-PCR assay revealed that the circ_0011292 level was distinctly down-regulated and the miR-433-3p level was prominently upregulated in tumor tissues from the sh-circ_0011292 group compared to the sh-NC group (Figure 7e). Moreover, circ_0011292 silence also decreased the mRNA and protein levels of CHEK1 (Figure 7e,f). Thus, it was concluded that circ_0011292 silence could suppress tumor growth in vivo at least partially relying on the circ_0011292/miR-433-3p/CHEK1 pathway.

DISCUSSION

Currently, the production of chemoresistance has become the major hindrance for NSCLC treatment.²⁰ CircRNAs with aberrant expression have been shown to take part in the process of carcinogenesis and chemoresistance development in NSCLC.^{21,22} In this study, we focused on digging into the biological function and underlying molecular basis of circ_0011292 in PTX-resistant NSCLC cell malignant progression. Moreover, the functional roles of the circ_0011292/miR-433-3p/CHEK1 network in regulating PTX resistance of NSCLC cells were identified.

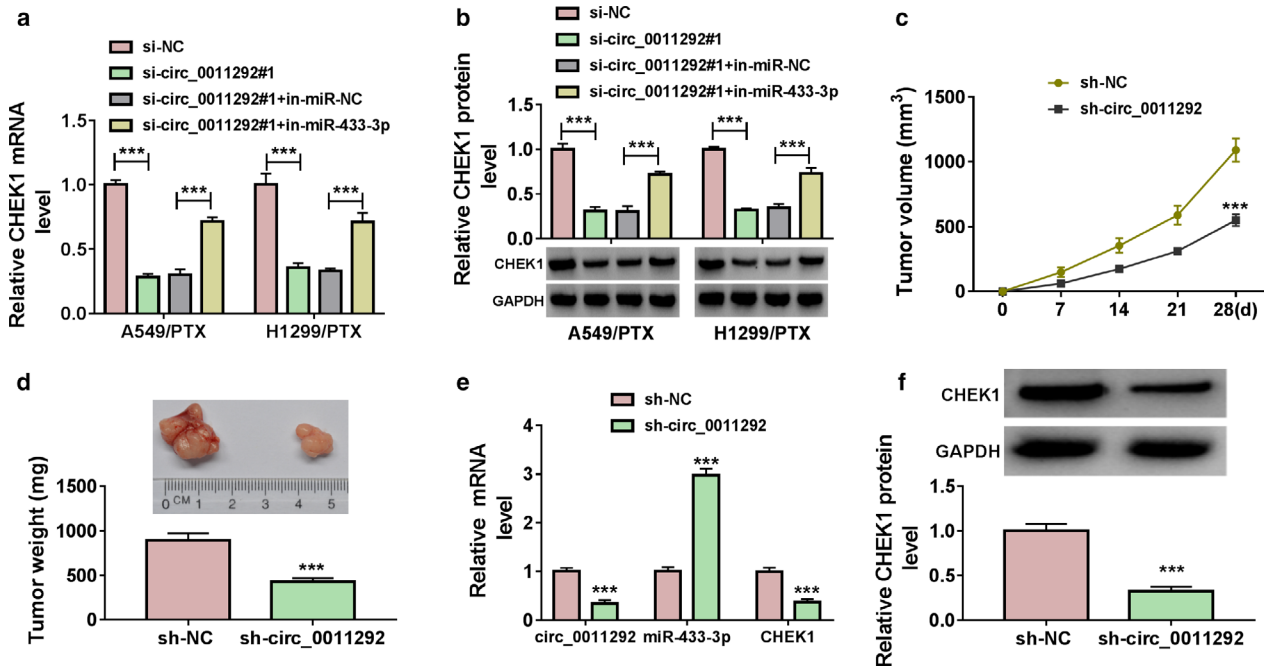


FIGURE 7 Knockdown of circ_0011292 blocked NSCLC tumor growth via circ_0011292/miR-433-3p/CHEK1 axis in vivo^{***}. (a and b) The mRNA and protein expression of CHEK1 in A549/PTX and H1299/PTX cells transfected with si-NC, si-circ_0011292#1, si-circ_0011292#1 + in-miR-NC or si-circ_0011292#1 + in-miR-433-3p was determined via qRT-PCR and Western blot assays, respectively. Xenograft tumor models were established using inoculating A549/PTX cells stably transfected with sh-circ_0011292 or sh-NC into nude mice. (c) Tumor volume was measured every 7 days using calipers. (d) Tumor weight was tested after 28 days of inoculation. (e) The levels of circ_0011292, miR-433-3p, and CHEK1 in the collected tumor tissues of xenograft mice were determined by qRT-PCR analysis. (f) Western blot was conducted for CHEK1 protein level in tumor tissues of xenograft mice. ^{***}*p* < 0.001

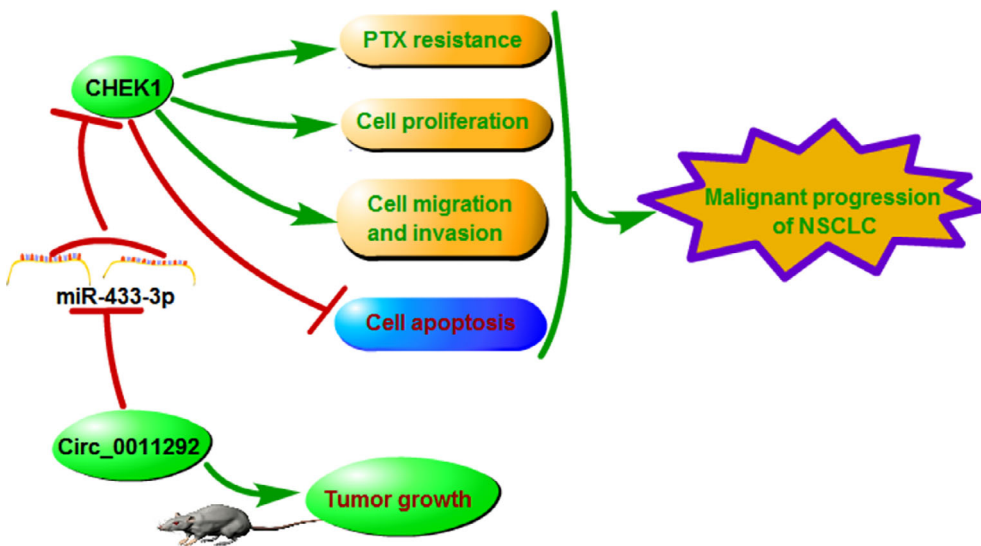


FIGURE 8 Schematic diagram showing circ_0011292-promoted PTX resistance, cell proliferation, migration, and invasion and inhibited apoptosis in PTX-resistant NSCLC cells

It is well documented that numerous circRNAs are crucial cancer-regulatory molecules in the pathogenesis and chemoresistance of NSCLC through playing their sponge effect on natural miRNAs and affecting the transcription-translation of genes.^{23,24} For instance, circ_0085131 facilitated cell proliferation and cisplatin resistance in NSCLC via regulating autophagy mediated by miR-654-5p/ATG7 pathway.²⁵ Meanwhile, circRNAs were dysregulated and modulated the resistance of NSCLC cells to taxol (PTX) and

exerted biological effects by absorbing and sequestering miRNA molecules.²² Recent research has ascertained that circ_0011292 enhanced PTX resistance and tumorigenesis by regulating the miR-379-5p/TRIM65 axis in NSCLC.¹⁰ Herein, it was found that circ_0011292 was highly expressed in NSCLC tissues and cells, especially in PTX-resistant NSCLC cells. Loss-of-function experiments showed that circ_0011292 deficiency rendered the sensitivity of PTX-resistant cells to PTX, and also distinctly repressed cell

proliferation, migration, invasion, and enhanced apoptosis in PTX-resistant NSCLC cells. From this evidence, it could be speculated that circ_0011292 serves as a novel oncogene and contributes to PTX resistance in NSCLC cells.

The ceRNA hypothesis supposes that circRNAs modulate gene expression through sequestering miRNAs, reducing their ability to target mRNAs.²⁶ Here, it was first highlighted that circ_0011292 directly targeted miR-433-3p and negatively regulated miR-433-3p expression in NSCLC cells. Meanwhile, miR-433-3p was downregulated in NSCLC tissues and cells, and it was further reduced in PTX-resistant NSCLC cells compared to parental cells. In accordance with our study, Weng et al. discovered that miR-433-3p was had low expression in NSCLC cells and miR-433-3p overexpression inhibited cell proliferation, migration, and invasion but accelerated cell apoptosis.¹⁵ Furthermore, our data suggested that miR-433-3p overexpression enhanced PTX sensitivity, restrained cell proliferation, migration, and invasion, and induced apoptosis in PTX-resistant NSCLC cells. Hence, we deemed that miR-433-3p was an anticancer factor in the progression of NSCLC. Moreover, miR-433-3p suppression effectively reversed the impacts of circ_0011292 deficiency on PTX resistance and cell malignant progression in PTX-resistant NSCLC cells in our study. This demonstrates that circ_0011292 improved the resistance of PTX-resistant NSCLC cells to PTX through sponging miR-433-3p.

To date, mounting miRNAs have been disclosed to exert essential regulatory roles in multiple human cancers, including NSCLC, through interaction with the 3'-UTRs of target mRNAs.²⁷ In addition, miR-433-3p has been shown to participate in the carcinogenesis of different malignancies via regulating downstream genes.^{28,29} For example, miR-433-3p was associated with renal carcinoma cell growth and migration by targeting FGF2,³⁰ and miR-433-3p overexpression markedly impeded cell proliferation, metastasis while expedited cell apoptosis in osteosarcoma.²⁸ Liu et al. have identified that miR-433 was significantly downregulated in NSCLC and the resumption of miR-433 expression inhibited the proliferation and invasion of NSCLC cells partly through directly sponging E2F transcription factor 3 (E2F3).³¹ Li et al. also showed the reduced expression of miR-433 in NSCLC and its repressive effects on repressive tumor progression via Smad2.³² Here, we also discovered the upregulation of CHEK1 in NSCLC tissues and cells, as well as PTX-resistant NSCLC cells. We are the first to identify that miR-433-3p directly targets CHEK1. Furthermore, as with circ_0011292, CHEK1 silence promoted PTX sensitivity, inhibited cell proliferation, migration, and invasion, and accelerated apoptosis in PTX-resistant NSCLC cells. In addition, CHEK1 elevation could counteract the suppression on IC50 of PTX, proliferation, migration, and invasion, and the promotion on apoptosis of A549/PTX and H1299/PTX cells with miR-433-3p overexpression, indicating that miR-433-3p enhanced PTX sensitivity by targeting CHEK1. More importantly, this is the first report on the role of

circ_0011292 as a miR-433-3p sponge to further control CHEK1 expression. The experimental animals in biomedical research provide insights into disease mechanisms, and BALB/c nude mice are mammalian animals that are widely used to establish animal models of human disease.³³ Herein, the xenograft model assay result also demonstrates that circ_0011292 blocks the NSCLC tumor growth via circ_0011292/miR-433-3p/CHEK1 axis in vivo. Thus, we speculated that circ_0011292 might participate in the progression of PTX-resistant NSCLC via sponging miR-433-3p and regulating CHEK1 expression.

In summary, we unraveled the dysregulation and role of circ_0011292, miR-433-3p, and CHEK1 in NSCLC tissues and PTX-resistant NSCLC cells. Circ_0011292 might contribute to the malignant development and PTX resistance of NSCLC cells in vitro through modulation of the miR-433-3p/CHEK1 axis (Figure 8). These findings might provide a strong theory for developing circ_0011292 as a potential therapeutic target for the remedy of chemoresistant NSCLC patients.

CONFLICT OF INTEREST

The authors declare that they have no financial conflicts of interest.

DATA AVAILABILITY STATEMENT

Please contact the correspondence author for the data request.

ORCID

Yong Zhang  <https://orcid.org/0000-0002-7805-8208>

REFERENCES

- Nasim F, Sabath BF, Eapen GA. Lung cancer. *Med Clin North Am.* 2019;103(3):463–73.
- Gridelli C, Rossi A, Carbone DP, Guarize J, Karachaliou N, Mok T, et al. Non-small-cell lung cancer. *Nat Rev Dis Primers.* 2015;1:15009.
- Holohan C, Van Schaeybroeck S, Longley DB, Johnston PG. Cancer drug resistance: an evolving paradigm. *Nat Rev Cancer.* 2013;13(10):714–26.
- Li XQ, Ren J, Wang Y, Su JY, Zhu YM, Chen CG, et al. Synergistic killing effect of paclitaxel and honokiol in non-small cell lung cancer cells through paraptosis induction. *Cell Oncol (Dordr).* 2020;44(1):135–50.
- Patop IL, Wust S, Kadener S. Past, present, and future of circRNAs. *EMBO J.* 2019;38(16):e100836.
- Xu T, Wang M, Jiang L, Ma L, Wan L, Chen Q, et al. CircRNAs in anticancer drug resistance: recent advances and future potential. *Mol Cancer.* 2020;19(1):127.
- Song L, Cui Z, Guo X. Comprehensive analysis of circular RNA expression profiles in cisplatin-resistant non-small cell lung cancer cell lines. *Acta Biochim Biophys Sin (Shanghai).* 2020;52(9):944–53.
- Pang J, Ye L, Zhao D, Zhao D, Chen Q. Circular RNA PRMT5 confers cisplatin-resistance via miR-4458/REV3L axis in non-small-cell lung cancer. *Cell Biol Int.* 2020;44(12):2416–26.
- Li X, Yang B, Ren H, Xiao T, Zhang L, Li L, et al. I_circ_0002483 inhibited the progression and enhanced the Taxol sensitivity of non-small cell lung cancer by targeting miR-182-5p. *Cell Death Dis.* 2019;10(12):953.
- Guo C, Wang H, Jiang H, Qiao L, Wang X. Circ_0011292 enhances paclitaxel resistance in non-small cell lung cancer by regulating miR-

- 379-5p/TRIM65 Axis. *Cancer Biother Radiopharm*. 2020. <https://doi.org/10.1089/cbr.2019.3546>
11. Di Leva G, Garofalo M, Croce CM. MicroRNAs in cancer. *Annu Rev Pathol*. 2014;9:287-314.
 12. Fabian MR, Sonenberg N, Filipowicz W. Regulation of mRNA translation and stability by microRNAs. *Annu Rev Biochem*. 2010;79:351-79.
 13. Sun H, Zhou X, Bao Y, Xiong G, Cui Y, Zhou H. Involvement of miR-4262 in paclitaxel resistance through the regulation of PTEN in non-small cell lung cancer. *Open Biol*. 2019;9(7):180227.
 14. Xu X, Jin S, Ma Y, Fan Z, Yan Z, Li W, et al. miR-30a-5p enhances paclitaxel sensitivity in non-small cell lung cancer through targeting BCL-2 expression. *J Mol Med*. 2017;95(8):861-71.
 15. Weng L, Qiu K, Gao W, Shi C, Shu F. LncRNA PCGEM1 accelerates non-small cell lung cancer progression via sponging miR-433-3p to upregulate WTAP. *BMC Pulm Med*. 2020;20(1):213.
 16. Xie Y, Wei RR, Huang GL, Zhang MY, Yuan YF, Wang HY. Checkpoint kinase 1 is negatively regulated by miR-497 in hepatocellular carcinoma. *Med Oncol*. 2014;31(3):844.
 17. Grabauskiene S, Bergeron EJ, Chen G, Chang AC, Lin J, Thomas DG, et al. CHK1 levels correlate with sensitization to pemetrexed by CHK1 inhibitors in non-small cell lung cancer cells. *Lung Cancer*. 2013;82(3):477-84.
 18. Liang L, Zhang L, Zhang J, Bai S, Fu H. Identification of circRNA-miRNA-mRNA networks for exploring the fundamental mechanism in lung adenocarcinoma. *Oncotargets Ther*. 2020;13:2945-55.
 19. Xu D, Wu Y, Wang X, Hu X, Qin W, Li Y, et al. Identification of functional circRNA/miRNA/mRNA regulatory network for exploring prospective therapy strategy of colorectal cancer. *J Cell Biochem*. 2020. <https://doi.org/10.1002/jcb.29703>
 20. Chang A. Chemotherapy, chemoresistance and the changing treatment landscape for NSCLC. *Lung Cancer*. 2011;71(1):3-10.
 21. Zhang PF, Pei X, Li KS, Jin LN, Wang F, Wu J, et al. Circular RNA circFGFR1 promotes progression and anti-PD-1 resistance by sponging miR-381-3p in non-small cell lung cancer cells. *Mol Cancer*. 2019;18(1):179.
 22. Xu N, Chen S, Liu Y, Li W, Liu Z, Bian X, et al. Profiles and bioinformatics analysis of differentially expressed Circrnas in Taxol-resistant non-small cell lung cancer cells. *Cell Physiol Biochem*. 2018;48(5):2046-60.
 23. Li YH, Xu CL, He CJ, Pu HH, Liu JL, Wang Y. circMTDH.4/miR-630/AEG-1 axis participates in the regulation of proliferation, migration, invasion, chemoresistance, and radioresistance of NSCLC. *Mol Carcinog*. 2020;59(2):141-53.
 24. Sun H, Chen Y, Fang YY, Cui TY, Qiao X, Jiang CY, et al. Circ_0000376 enhances the proliferation, metastasis, and chemoresistance of NSCLC cells via repressing miR-384. *Cancer Biomark*. 2020;29(4):463-73.
 25. Kong R. Circular Rlhasa_circ_0085131 is involved in cisplatin-resistance of non-small-cell lung cancer cells by regulating autophagy. *Cell Biol Int*. 2020;44(9):1945-56.
 26. Hansen TB, Jensen TI, Clausen BH, Bramsen JB, Finsen B, Damgaard CK, et al. Natural RNA circles function as efficient micro-RNA sponges. *Nature*. 2013;495(7441):384-8.
 27. Wang XW, Guo QQ, Wei Y, Ren KM, Zheng FS, Tang J, et al. Construction of a competing endogenous RNA network using differentially expressed lncRNAs, miRNAs and mRNAs in nonsmall cell lung cancer. *Oncol Rep*. 2019;42(6):2402-15.
 28. Hou XK, Mao JS. Long noncoding RNA SNHG14 promotes osteosarcoma progression via miR-433-3p/FBXO22 axis. *Biochem Biophys Res Commun*. 2020;523(3):766-72.
 29. Shi Q, Wang Y, Mu Y, Wang X, Fan Q. MiR-433-3p inhibits proliferation and invasion of esophageal squamous cell carcinoma by targeting GRB2. *Cell Physiol Biochem*. 2018;46(5):2187-96.
 30. Cai X, Zhang X, Mo L, Zhu J, Yu H. LncRNA PCGEM1 promotes renal carcinoma progression by targeting miR-433-3p to regulate FGF2 expression. *Cancer Biomark*. 2020;27(4):493-504.
 31. Liu N, Liu Z, Zhang W, Li Y, Cao J, Yang H, et al. MicroRNA433 reduces cell proliferation and invasion in nonsmall cell lung cancer via directly targeting E2F transcription factor 3. *Mol Med Rep*. 2018;18(1):1155-64.
 32. Li J, Chen M, Yu B. miR-433 suppresses tumor progression via Smad2 in non-small cell lung cancer. *Pathol Res Pract*. 2019;215(10):152591.
 33. Yong KSM, Her Z, Chen Q. Humanized mice as unique tools for human-specific studies. *Arch Immunol Ther Exp (Warsz)*. 2018;66(4):245-66.

How to cite this article: Jin M, Zhang F, Li Q, Xu R, Liu Y, Zhang Y. Circ_0011292 knockdown mitigates progression and drug resistance in PTX-resistant non-small-cell lung cancer cells by regulating miR-433-3p/CHEK1 axis. *Thorac Cancer*. 2022;13:1276-88. <https://doi.org/10.1111/1759-7714.14378>